Applied Catalysis B: Environmental 136–137 (2013) 294–301

Contents lists available at SciVerse ScienceDirect

Applied Catalysis B: Environmental

journal homepage: www.elsevier.com/locate/apcatb

Synergistic catalytic degradation of antibiotic sulfamethazine in a heterogeneous sonophotolytic goethite/oxalate Fenton-like system

Tao Zhou[a,**], Xiaohui Wu[a], Yanrong Zhang[a], Jianfeng Li[b], Teik-Thye Lim[c,d,*]

[a] School of Environmental Science and Engineering, Huazhong University of Science and Technology, Wuhan, 430074, PR China
[b] Institute of Environmental Science & Engineering, Nanyang Technological University, 7 Nanyang Drive, Singapore 639732, Republic of Singapore
[c] School of Civil and Environmental Engineering, Nanyang Technological University, 50 Nanyang Avenue, Singapore 639798, Republic of Singapore
[d] Nanyang Environment & Water Research Institute (NEWRI), Nanyang Technological University, 1 Cleantech Loop, CleanTech One, Singapore 637141, Republic of Singapore

ARTICLE INFO

Article history:
Received 18 October 2012
Received in revised form 25 January 2013
Accepted 3 February 2013
Available online 11 February 2013

Keywords:
Sonophotocatalysis
Fenton-like
Sulfamethazine
Iron–oxalate complexes
Goethite

ABSTRACT

A novel heterogeneous sonophotolytic goethite/oxalate Fenton-like (SP-FL) system was developed in this study. Compared to the corresponding photochemical Fenton-like (P-FL) system and sonochemical Fenton-like system (S-FL) system, it was found that the SP-FL system could achieve synergistic degradation of antibiotic sulfamethazine (SMZ). A synergy factor of 2.2 based on pseudo-first-order degradation rate constant (k_{obs}) was observed, along with great improvements in organic mineralization and wastewater detoxification. Examining the evolution of dissolved iron species and reactive oxygen species (H_2O_2 and •OH) in the three systems revealed that the SMZ degradation strongly relied on the "in-situ" photochemical generation of H_2O_2 and fast regeneration of dissolved Fe(II) species. Identification of the organic intermediates and released inorganic ions suggested that the cleavage of S—N bond in the SMZ molecule was dominant under •OH attacking. The important synergistic role of ultrasound (US) in promoting SMZ degradation was proposed. Herein US could affect the system at multi-folds: (1) accelerating the goethite-chelating dissolution by reducing mass transfer barriers, (2) enhancing the radical reactions in the bulk solution with sonochemical cavitation effect, and (3) possible direct hydrolysis of amine intermediates inside the cavitation bubbles.

1. Introduction

As a typical class of antibiotics, sulfonamides are widely used in human and veterinary medicine as antibacterial drugs and growth promoters [1]. Moreover, it has been reported that the ubiquitous appearance of sulfonamides and their metabolites could be easily found in the surrounding aquatic environment [1–3]. Listed as pseudo-persistent pollutants, sulfonamides residuals have become one of the most concerned issues due to their potential adverse effects on human beings and the aquatic ecological environment [1,4].

Advanced oxidation processes (AOPs) have been proposed in the past decades as effective alternatives for degrading many toxic and biorefractory organic pharmaceuticals [5]. As one of the classic AOPs, Fenton reaction (or Fenton reagent) which generally contains a series of reactions between ferrous and H_2O_2 has been well investigated and established as an effective method for organic pharmaceuticals destruction [5]. However, in a traditional Fenton reaction system, the free ferrous is rapidly consumed initially, requiring step-wise addition of Fe^{2+} and resulting in its accumulation in effluents. Moreover, the direct use of unstable H_2O_2 is also a challenge to practical industrial applications of Fenton reaction.

The use of iron oxides (or iron minerals) in catalyzing Fenton reaction has received increasing investigations since these iron minerals are naturally available and easily separated from bulk solutions. It is reported that these so-called heterogeneous Fenton-like reaction systems could be also capable of efficiently degrading numerous pharmaceuticals [6]. Although different iron oxides have been used in previous studies, generally the rate-determining steps could be mainly ascribed to the solid–water surface interaction, i.e. iron dissolution from the solid (iron oxides) surface to the bulk solution.

Organic ligands, such as oxalate, citrate, tartarate and EDTA, are usually used to enhance either homogeneous Fenton reaction or heterogeneous Fenton-like systems, since they could prevent the precipitation of dissolved iron species from the bulk solution and/or enhance the dissolution of iron oxides [7–10]. Most interestingly, the phenomena of "in-situ" H_2O_2 production have

* Corresponding author at: School of Civil and Environmental Engineering, Nanyang Technological University, 50 Nanyang Avenue, Singapore 639798, Republic of Singapore. Tel.: +65 67906933; fax: +65 67910676.
** Corresponding author. Tel.: +86 27 87792101; fax: +86 27 87792101.
E-mail addresses: zhoutao@hust.edu.cn (T. Zhou), cttlim@ntu.edu.sg (T.-T. Lim).

0926-3373/$ – see front matter © 2013 Elsevier B.V. All rights reserved.
http://dx.doi.org/10.1016/j.apcatb.2013.02.004

been found in different ligand-based systems, e.g. photolytic Fe(III)–oxalate and Fe^0/EDTA/air systems [11–14]. The photolytic Fe(III)–oxalate systems, either in homogenous or in heterogeneous forms, has attracted a great deal of scientific attention [12,15–23] since the study published by Zuo and Hoigne [24]. Together with photolysis (UV or visible light), Fe(III)–oxalate complexes could promote the formation of Fe(II) species homogeneously. In addition, Fenton reaction catalyzed by Fe(II)–oxalate complexes could increase hydroxyl radicals (•OH) generation rate which was approximately 3–4 orders of magnitude higher than that achieved in traditional Fenton reaction system [15,17]. Light-irradiated heterogeneous Fe(III)/oxalate systems could also achieve high efficiencies in degrading organic contaminants. Previous researchers have reported that diuron and pentachlorophenol could be rapidly degraded by using goethite [23] and maghemite [12] as the Fenton reaction catalysts, respectively.

Ultrasound (US) technology is a very useful technique for improving the reaction efficiency of Fenton systems, especially heterogeneous Fenton-like systems since the presence of solid particles in the aqueous system was found to enhance the production of sonochemical microbubbles [25,26]. On the other hand, Katsumata et al. [27] has reported that the significant synergistic degradation and mineralization of fenitrothion could be achieved in a US/ferrioxalate/UV process. In a previous study, we also concluded that US played profound enhancement roles in different sonophotolytic Fe(III)–ligand systems [28]. However, to our best knowledge, degradations of organic pollutants and explanations of their related reaction mechanisms or US enhancement roles in heterogeneous sonophotolytic Fe(III)–ligand systems are still scarce.

Therefore, in the present study, we have investigated the degradation of a selected sulfonamide–sulfamethazine (SMZ) in a sonophotolytic goethite/oxalate Fenton-like system. The objectives were to: (1) examine the synergistic degradation of SMZ in the sonophotolytic Fenton-like system and evaluate affecting experimental parameters; (2) study the degradation products and propose possible degradation pathways; and (3) clarify the reaction mechanism in the system and reveal the promotional role of US in the overall process.

2. Materials and methods

2.1. Chemicals

All chemicals were used as received without further purification. Millipore Co. MilliQ (MQ) water with resistivity of 18.2 MΩ cm was used throughout the study unless otherwise stated. Purified (>99%) sulfamethazine, oxalic acid and were obtained from Singapore Sigma–Aldrich and Merck Company, respectively. Other used chemicals, goethite (~35% Fe), NaOH, $HClO_4$, $NaClO_4$ and the reagents for sample analysis, were all purchased from Singapore Sigma–Aldrich.

2.2. Methods

A 600 mL jacket glass reactor, which was equipped with an UV lamp and an US probe inside, was utilized and the reaction temperatures were maintained at $20 \pm 1\,^{\circ}C$ by circulating cooling water. UVA irradiation was provided by a 9 W UVA lamp (NEC FL8 BL-B, $\lambda_{max} = 365$ nm) and the light intensity was 7.7 ± 0.1 mW cm^{-2} (VECTOR H410 radiometer, Scientech Boulder CO., USA). Continuous ultrasonic shockwave was emitted by a sonicator at a fixed frequency of 20 kHz (XL2020, Misonix Incorporated, New York, USA). During the reaction, purified air was supplied into the reactor through a glass diffuser at 1.0 L min^{-1} and the solution was well magnetic-mixed (700 rpm).

In a typical experimental run, an aqueous suspension containing the desired initial concentrations of SMZ (25 mg L^{-1}), goethite (0.5 g L^{-1}) and oxalic acid (0.8 mM) was prepared in dark. Initial pH was adjusted to 3 by using 0.1 M $HClO_4$ or NaOH, and the solution ion strength (I) was adjusted to 0.1 by 0.1 M $NaClO_4$. After mixing at least for 30 min to achieve equilibrium of the solid dissolution and iron–ligands chelation, the reaction was commenced by switching on the lamp and sonicator simultaneously. Samples were withdrawn at specific time intervals and analyzed immediately after filtration through 0.45 μm membrane.

2.3. Analysis

Quantitative analysis of SMZ and oxalate was performed with HPLC (WATERS 2695) equipped with a XTerra C18 column and a photodiode array detector (WATERS 2996). For the analysis of SMZ, the mobile phase was a mixture of methanol and MQ water (V/V = 40%:60%) at a flow rate of 0.5 mL min^{-1}. The detector wavelength was set at 260 nm. For the analysis of oxalic acid, the mobile phase was a mixture of 20 mmol KH_2PO_4 buffer (pH 2.2) and acetonitrile (V/V = 95%:5%) at a flow rate of 1 mL min^{-1} and the determined wavelength was set at 220 nm.

Identification of organic intermediates was performed with a gas chromatograph (Agilent 6890, USA) equipped with a 30 m × 0.25 μm HP5 column and mass selective detector. Before GC/MS analysis, predetermined 250 mL sample was concentrated by using C18 extraction columns (HLB, Waters Oasis®). The GC/MS column temperature was programmed from 60 °C (held for 2 min) to 285 °C (held for 2 min) at a rate of 10 °C min^{-1}. Injector and detector temperatures were 200 and 220 °C respectively. Helium was used as the carrier gas at a flow rate of 0.8 mL min^{-1} and 1 μL sample injections were accomplished in split mode. MS was operated in electron ionization mode (70 eV) and the spectra were obtained at a scan range from m/z 33–500 with a scan time of 0.3 s and interscan of 0.01 s.

Total organic carbon (TOC) was measured by a Shimadzu TOC analyzer (TOC-500, Singapore). The luminescent marine bacteria *Vibrio fischeri* were used to evaluate the acute ecotoxicity of water samples, measuring by a Microtox 500 Analyzer (SDI, USA). The procedure has been described elsewhere [28].

The concentration of H_2O_2 was measured spectrophotometrically using the DPD (N,N-diethyl-p-phenylenediamine) method [29]. The determination of accumulated concentration of •OH radical was conducted by HPLC, following a dimethyl sulfoxide (DMSO) trapping method [30]. By using this method, the concentration of •OH is indirectly quantified with an indicative compound (DNPH–HCHO) which is formed by the reaction between 2,4-dinitrophenyl-hydrazine (DNPH) and the adduct of •OH radicals and DMSO. The *o*-phenanthroline colorimetric method ($\lambda = 510$ nm, $\varepsilon = 1.1 \times 10^4$ M^{-1} cm^{-1}) was used to identify the concentration of generated ferrous ion. The total dissolved iron concentrations were determined by using an inductively coupled plasma-optical emission spectrometry (ICP-OES, Optima 2000DV, PerkinElmer Instruments). Then the concentrations of dissolved Fe(III) species could be calculated as $C_{Fe}{}^{(III)} = C_{Total\ Fe} - C_{Fe}{}^{(II)}$.

The released inorganic anions (sulfate, nitrate and nitrite) were monitored by a Dionex ICS-1000 ion chromatography (IC) system equipped with a conductivity detector. An IonPac AS15 anion-exchange column (4 mm × 250 mm) was employed with an elution containing 36 mM KOH at a flow rate of 1.2 mL min^{-1}. Ammonium (NH_4^+) was determined using the colorimetric nesslerization method (HACH Method 8038) with a HACH DR/2400 spectrophotometer.

Characterizations of solid surface were conducted by using JEOL JSM6360 Scanning Electron Microscope (SEM). X-ray diffraction (XRD) patterns were obtained from a Bruker D8 ADVANCE X-ray

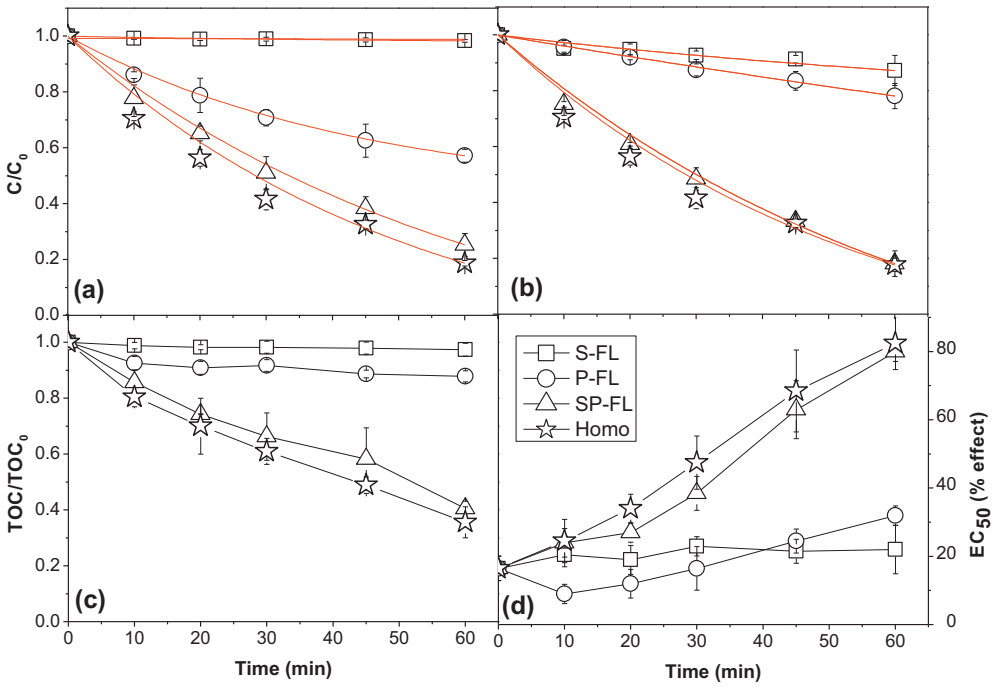

Fig. 1. Degradation efficiencies in the different systems versus the reaction time (a) SMZ degradation; (b) oxalate decomposition, (c) TOC removal, and (d) acute toxicity EC_{50} (initial parameters: 25 mg L^{-1} SMZ, 0.5 g L^{-1} goethite, 0.8 mM oxalic acid, 330 W US input power and pH 3). "Homo" in the figure stands for the corresponding homogeneous SP-FL system (US/UV/Fe^{3+}-Oxa) with an initial Fe^{3+} concentration of 250 μM. Error bars represent 95% confidence limits.

diffractometer with Cu Kα radiation (λ = 1.5418 Å) in a 2θ range of 5–80°. The crystallite size and anatase content were obtained from TOPAS 2.0 software. Before the characterization operations, related solids taken from the reactor were washed by deionized water and dried in a vacuum freeze-dryer overnight.

3. Results and discussions

3.1. Synergistic SMZ degradation achieved in the heterogeneous SP-FL system

As shown in Fig. 1, it was demonstrated that a significant synergistic degradation of SMZ could be achieved in the heterogeneous sonophotolytic goethite/oxalate Fenton-like system (SP-FL) system, as compared to that achieved in the corresponding sonochemical Fenton-like system (S-FL) and the photolytic Fenton-like system (P-FL) respectively. From Fig. 1a, it could be concluded that the pseudo-first order degradation kinetic could be well applied in the three systems. The corresponding k_{obs}(SMZ) values are listed in Table 1. According to Eq. (1) modified from a previous paper [31], a synergy factor of SMZ degradation in the SP-FL system can be concluded as 2.2.

$$\text{synergy factor} = \frac{k_{\text{US/UV/goethite-oxalate}}}{(k_{\text{UV/goethite-oxalate}} + k_{\text{US/goethite-oxalate}})} \quad (1)$$

As depicted in Fig. 1b, it was found that oxalate could be simultaneously degraded with the SMZ decomposition. The degradation of oxalate could be also applied with the pseudo-first order kinetic. The values of the related k_{obs}(oxalate) in three systems are presented in Table 1. Apparently, the SP-FL system led to a much faster decomposition rate of oxalate than the other two systems.

Significant mineralization enhancement in the SP-FL system was also observed. After 1 h of reaction time, 60% of TOC was removed in the SP-FL system, whereas only insignificant (<3%) and 12% of TOC were removed in the S-FL system and the P-FL system, respectively (Fig. 1c). Furthermore, the SP-FL system could also lead to a rapid detoxification (decrease of the acute ecotoxicity) of the synthetic wastewater. As shown in Fig. 1d, it is found that the EC_{50} value in the SP-FL system was increased from 16.5% (before reaction) to 80% after the treatment while its change in the S-FL system was insignificant. It was noted that an initial increase of acute ecotoxicity followed by gradual decrease of the EC_{50} value was observed in the P-FL system. This implied the initial appearance of some organic intermediates with higher acute toxicity than SMZ. Thereafter, these organic intermediates would be gradually mineralized, subsequently leading to a continuous decrease of the acute ecotoxicity of the treated solution. In addition, it can be also seen in Fig. 1 that the homogeneous SP-FL (US/UV/Fe^{3+}-Oxa) system achieved similar but slight higher degradation efficiencies for SMZ, oxalic acid, TOC and ecotoxicity, as compared to the corresponding heterogeneous SP-FL system. It indicated that the homogenous Fenton-like reactions were dominant in either homogenous or heterogeneous systems, also evidencing the improvement of ultrasound in heterogeneous inter-phase mass transfer.

3.2. Changes of the catalyst surface in the different systems

Fig. 2 shows the XRD patterns of the fresh and used solid catalysts in three different systems. The XRD pattern of the fresh catalyst (goethite) is similar to pure goethite pattern reported in the XRD standard data base library, and depicts the goethite of well crystalline [32]. After 1 h of reaction time in the P-FL system, it was found that most peaks of goethite has disappeared, implying that the reacted catalyst surface maybe covered by some amorphous iron hydroxides [33]. Moreover, it was interesting to note that approximately all the characteristic peaks of the goethite surface remained after its reaction in both the S-FL system and SP-FL system. This could be ascribed to the strong ultrasonic surface cleaning effect which would continuously regenerate the catalyst surface throughout the whole reaction.

The SEM morphologies of the fresh and used catalysts are shown in Fig. 3. It evidences that the surface of used goethite either the S-FL

Table 1
Summary of degradation efficiencies achieved in the different systems.

	k_{obs}(SMZ)[a] ($\times 10^{-2}$ min^{-1})	R^2	k_{obs}(Oxalate)[b] ($\times 10^{-2}$ min^{-1})	R^2	k_{accum}(•OH)[c] ($\times 10^{-6}$ mol L^{-1} min^{-1})	R^2	Mineralization ratio (%)	EC_{50} (% effect)
S-FL	0.30 ± 0.14	0.903	0.23 ± 0.08	0.905	0.20	0.973	2.6 ± 2.3	22.0 ± 7.1
P-FL	1.0 ± 0.13	0.963	0.41 ± 0.10	0.997	1.3	0.988	12.1 ± 2.0	32.0 ± 2.8
SP-FL	2.2 ± 0.28	0.996	2.7 ± 0.21	0.985	2.5	0.987	59.5 ± 2.7	80.0 ± 2.8
Homo[d]	2.7 ± 0.11	0.987	2.9 ± 0.20	0.994	2.8	0.992	64.4 ± 5.5	82.5 ± 10.6

R^2 coefficients for the related calculated rate constants.
[a] Observed first-order degradation kinetic constants (k_{obs}) of SMZ.
[b] Observed first-order degradation kinetic constants (k_{obs}) of oxalate.
[c] Zero-order accumulation rate constant of •OH (obtained in the absence of SMZ).
[d] "Homo" stands for the corresponding homogeneous SP-FL system (US/UV/Fe^{3+}-Oxa) with an initial Fe^{3+} concentration of 250 μM. Error bars represent 95% confidence limits.

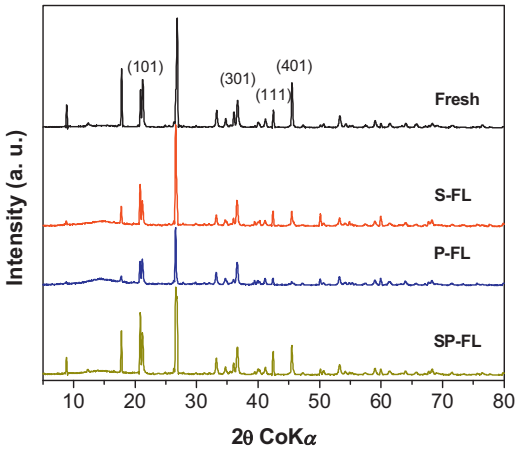

Fig. 2. XRD patterns of goethite after different treatments.

system or SP-FL system were strongly cleaned after 1 h of US irradiation, whereas the used catalyst without US treatment (i.e. treated by the P-FL system) had its surface covered by some anonymous iron oxides (Fig. 3b). As reported by Muruganandham et al. [26], US irradiation could increase not only the BET surface area but also the pore size and volume of goethite. It suggested possible successive recycling of the catalyst in the SP-FL system.

3.3. Evolution of dissolved iron species and reactive species in the different systems

Fig. 4a presents the evolution of dissolved iron species during the reaction in the three systems. At the beginning of the reaction in the P-FL and SP-FL systems, Fe(II) species were produced rapidly and then their amount slowly decreased throughout the reaction. However, it was found that there was a very slow rate of Fe(III) species reduction to Fe(II) species during the whole reaction time in the S-FL system. It indicated that the photolysis of iron(III)–oxalate complexes could lead to rapid regeneration of Fe(II) species, ensuring Fenton reaction sustainable at high rates (Eq. (2)). While in the S-FL system, due to the absence of sufficient Fe(II), a Fe(III) catalyzed

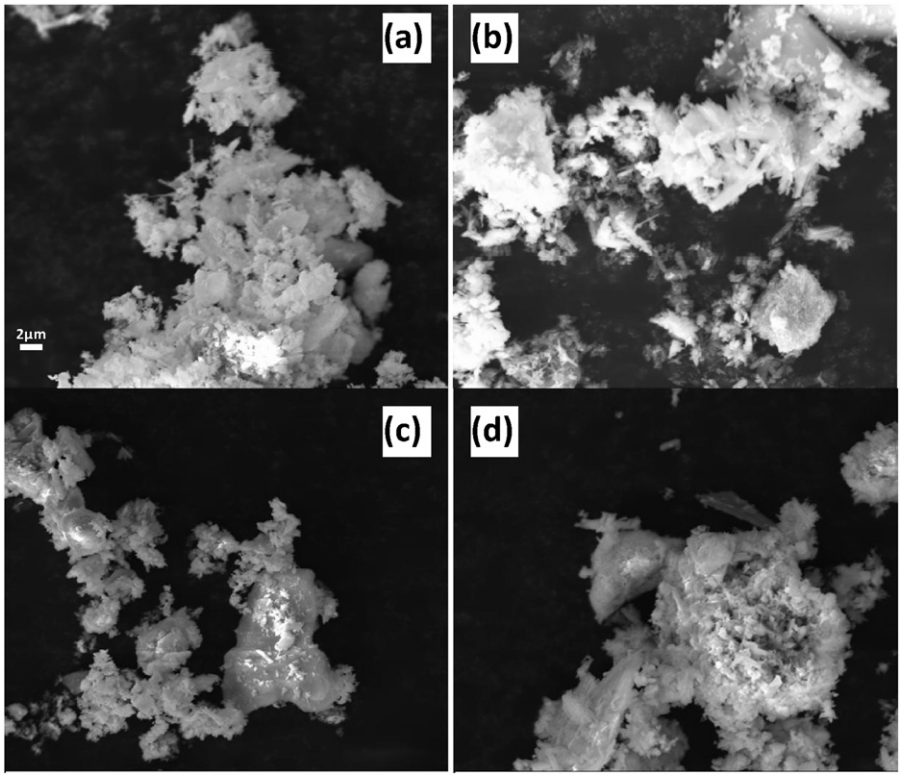

Fig. 3. SEM images of goethite surface after different treatments with 1 h of reaction time (a) Fresh, (b) S-FL, (c) P-FL and (d) SP-FL.

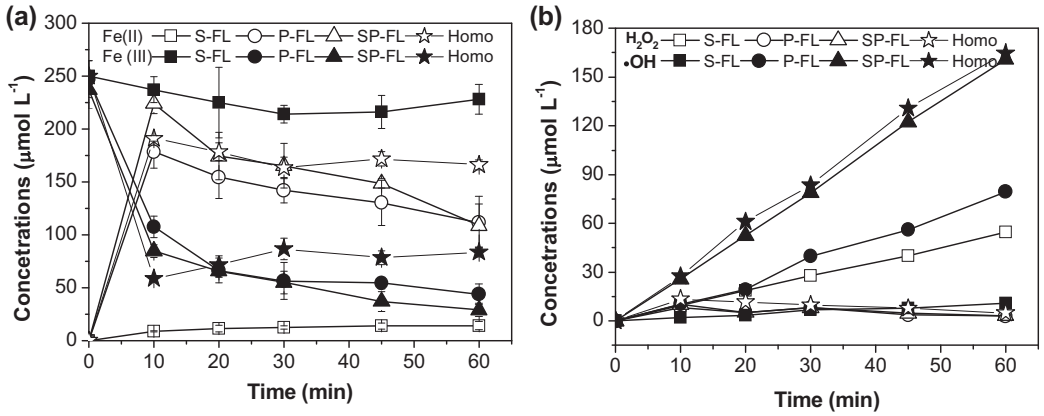

Fig. 4. Evolution of the concentrations of (a) dissolved iron species and (b) main reactive species (H_2O_2 and •OH) with elapsed reaction time in the different systems (initial parameters: 25 mg L^{-1} SMZ, 0.5 g L^{-1} goethite, 0.8 mM oxalic acid, 330 W US input power and pH 3). "Homo" in the figure stands for the corresponding homogeneous SP-FL system (US/UV/Fe^{3+}-Oxa) with an initial Fe^{3+} concentration of 250 μM. Error bars represents 95% confidence limits.

Fenton-like reaction which is a slow process occurred (Eq. (3)) [34]. It should be the main reason for the marginal SMZ degradation in the S-FL system (Fig. 1a).

$$Fe^{2+} + H_2O_2 \rightarrow Fe^{3+} + {}^{\bullet}OH + OH^-, \quad k = 76\,M^{-1}\,s^{-1} \qquad (2)$$

$$Fe^{3+} + H_2O_2 \rightarrow Fe^{2+} + HO_2{}^{\bullet}/O_2{}^{\bullet-} + H^+, \quad k = 0.01\,M^{-1}\,s^{-1} \qquad (3)$$

The distribution of Fe(III) and Fe(II) speciation in the presence of oxalate is a important factor in affecting the organics degradation in both the P-FL system and the SP-FL system [12,28]. The speciation of iron species and iron–oxalate complexes depends on pH and $C_2O_4{}^{2-}$ concentration as the amount of oxalic acid is excessive. Lan et al. [12] has reported that $Fe(C_2O_4)_2{}^-$ and $Fe(C_2O_4)_3{}^{3-}$, as well as Fe^{2+} and $Fe(C_2O_4)_2{}^{2-}$, were the main Fe(III) species and Fe(II) species respectively. In the case of SP-FL system, it was observed that pH increased (data not shown) with the rapid degradation of oxalic acid. Under this condition, $Fe(C_2O_4)_2{}^-$ and Fe^{2+} could be recognized as the dominant Fe(III) and Fe(II) species. In addition, we observed a decrease in the total amount of dissolved iron species with the elapsed reaction time, although this trend did not show obvious correlation with the oxalic acid degradation.

Quantification of the two main reactive species produced in the three systems as a function of reaction time was conducted in the absence of SMZ. As shown in Fig. 4b, a gradual increase in H_2O_2 concentration reaching 55 μmol L^{-1} at 1 h was found in the S-FL system, while the fluctuation of the H_2O_2 concentration at low level was observed in both the P-FL and SP-FL systems. Apparently, throughout the whole reaction, the H_2O_2 produced in the latter two systems could be rapidly decomposed in the presence of sufficient Fe(II) species (Fig. 4a). It could be also expected that the simultaneous faster regeneration of Fe(II) species would result in intense Fenton reaction in the SP-FL system, since the US irradiation could generate additional H_2O_2 in the SP-FL system as compared to the P-FL system.

As a direct product of Fenton reaction (Eq. (3)), •OH would be continuously produced. Fig. 4b also presents the •OH accumulation with the elapsed reaction time in the three different systems. The generated •OH versus reaction time could be well fitted with the zero-order accumulation kinetics. Table 1 shows the related kinetic constants (k_{accum}(•OH)) values. The highest accumulation rate obtained in the SP-FL system is well correlated with the synergistic efficiency in degrading SMZ, indicating •OH as the main oxidant.

The changes in the concentrations of dissolved iron species and the reactive species are shown in Fig. 4. It could be concluded that the •OH accumulation rate was similar to that achieved in the heterogeneous SP-FL system, corresponding to the evolution of dissolved iron species (Fig. 4a). In the homogenous SP-FL system, almost all the iron species remained in the solution at the end of reaction time. The result was different from that achieved in the heterogeneous SP-FL system in which the total dissolved iron concentration decreased in the end of reaction. It indicated the advantage of heterogeneous SP-FL system in wastewater treatment applications, since it would lower the environmental concern of dissolved iron from effluents discharged.

3.4. Intermediates, products and proposed degradation pathway in the SP-FL system

Identification of the released inorganic ions and organic intermediates could be helpful to gain insights into the SMZ degradation pathway in the SP-FL system. Fig. 5 shows the conversion fractions of organic sulfur and nitrogen containing in the SMZ molecule versus the reaction in the three systems. The most rapid release of the respective inorganic ions was observed in the SP-FL system, which was in accordance with its best SMZ degradation and mineralization ratio achieved (Fig. 1). Furthermore, it can be seen that the conversion of organic sulfur to $SO_4{}^{2-}$ was very efficient, while the conversion of organic nitrogen to the inorganic nitrogen ions such as $NH_4{}^+$, $NO_2{}^-$ and $NO_3{}^-$ was less efficient. This trend is similar to that achieved in a photocatalytic system [35], implying that the •OH attack occurs predominantly by addition to the benzene ring in the sulfanilic acid portion of the SMZ molecule, followed by the cleavage of S—N bond and production of nitrogen-containing organic intermediates as well as release of sulfate ion.

In fact, it has been reported that different sulfonamides would be transformed similarly under the •OH oxidation, even if the formed intermediates were of different stability according to their specific molecular structures [36,37]. In this study, two organic intermediates with the *m*/*z* of 294 and 123 have been identified during the reaction in the SP-FL system. According to the SMZ molecular structure, the related intermediates could be assigned to hydroxyl-sulfamethazine ($C_{12}H_{14}N_4O_3S$) and 4,6-2methyl-2-aminopyrimidine ($C_6H_9N_3$), respectively. This result evidenced that the cleavage of S—N bond in the SMZ molecule was dominant under •OH attacking. A SMZ degradation pathway in the SP-FL system could be then proposed (Fig. 6). With continuous •OH oxidation, the two main organic intermediates would be further decomposed, thus leading to the formation of low molecule weight amines, $NH_4{}^+$ and $NO_3{}^-$. Interestingly, the SP-FL system resulted in

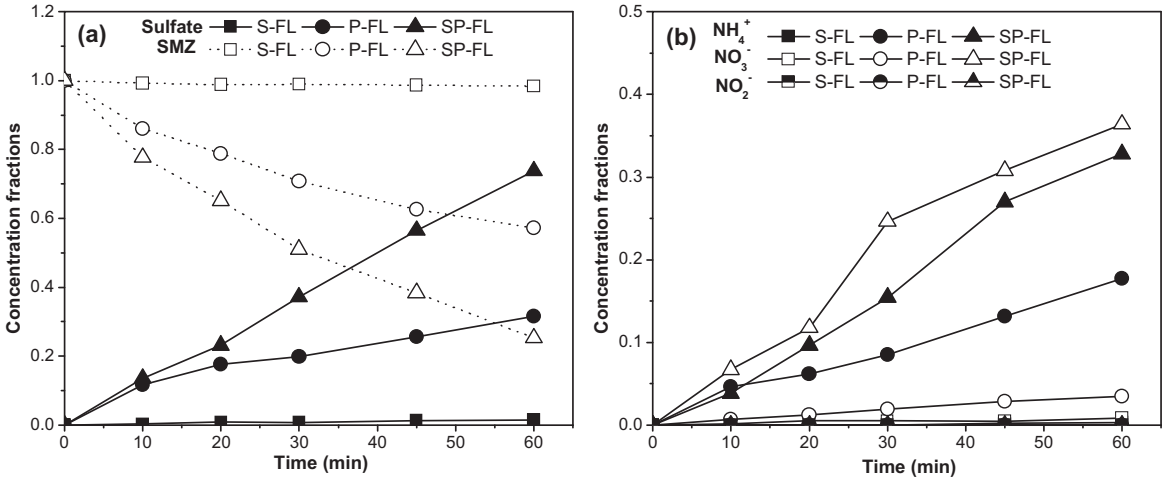

Fig. 5. The evolution of released inorganic ions during the SMZ degradation in the three systems (a) sulfate (b) inorganic nitrogen ions (initial parameters: 25 mg L^{-1} SMZ, 0.5 g L^{-1} goethite, 0.8 mM oxalic acid, 330 W US input power and pH 3). Error bars represent 95% confidence limits. The dot line in (a) represents the correlation of SMZ disappearance vs. sulfate released.

much higher NO_3^-/NH_4^+ mole ratios throughout the SMZ degradation (Fig. 5b), while only a corresponding ratio of 10:1 was reported in a photocatalytic system after 3 h illumination [35]. Since low NO_3^-/NH_4^+ ratios was found in the P-FL system (Fig. 5b), it can be concluded that US cavitation effect could favor and accelerate the oxidative transformation of amine intermediates into nitrate.

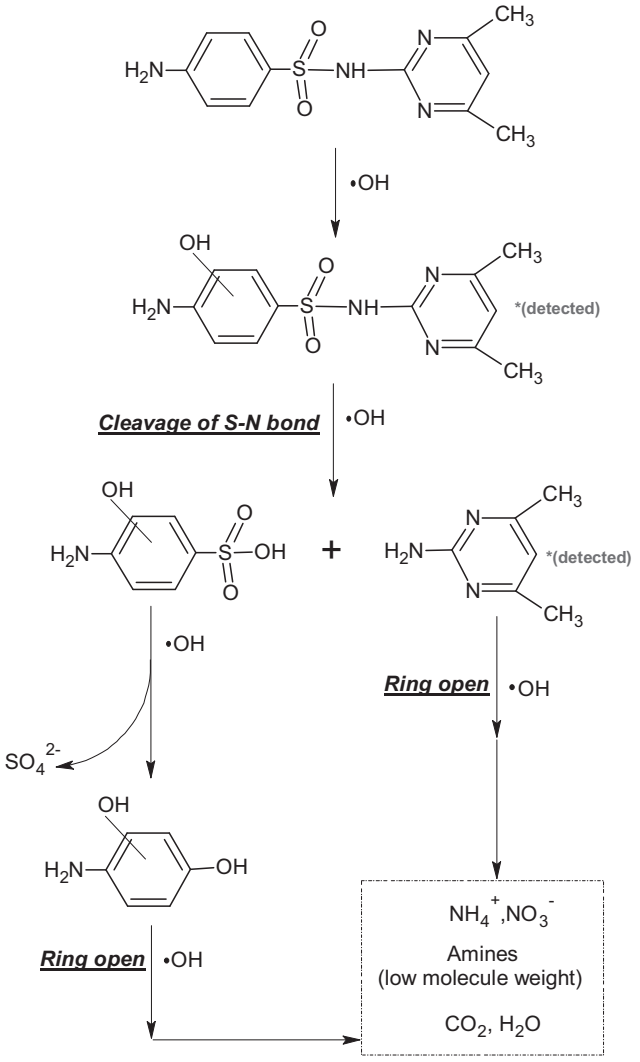

Fig. 6. Proposed SMZ degradation pathways in the SP-FL system.

3.5. Reaction mechanism in the SP-FL system and the promotional role of US

The mechanism of in situ H_2O_2 generation in irradiated iron–oxalate systems has already been clearly addressed in many studies [15,23]. Therein, the photoreduction of Fe(III)–oxalate complexes ($Fe^{(III)}[(C_2O_4)_n]^{3-2n}$) could trigger a series of reactions to produce additional H_2O_2, as depicted in Eqs. (4)–(9). In addition, these reactions simultaneously regenerate ferrous species ($Fe^{(II)}[(C_2O_4)_n]^{3-2n}$) at a faster rate than the direct photoreduction of Fe^{3+} to Fe^{2+}. Based on that, rapid oxidative degradation of target pollutants could be expected in the system.

$$Fe^{(III)}[(C_2O_4)_n]^{3-2n} + h\nu \rightarrow Fe^{(II)} + (n-1)C_2O_4^{2-} + C_2O_4^{\bullet-} \quad (4)$$

$$C_2O_4^{\bullet-} + O_2 \rightarrow 2CO_2 + O_2^{\bullet-} \quad (5)$$

$$O_2^{\bullet-} \leftrightarrow HO_2^{\bullet}\,(\text{pH dependent}) \quad (6)$$

$$O_2^{\bullet-}/HO_2^{\bullet} + H^+ \rightarrow H_2O_2 + O_2 \quad (7)$$

$$O_2^{\bullet-}/HO_2^{\bullet} + H^+ + Fe^{2+} \rightarrow H_2O_2 + O_2 + Fe^{3+} \quad (8)$$

$$Fe^{(II)}[(C_2O_4)_n]^{3-2n} + H_2O_2 \rightarrow Fe^{(III)}[(C_2O_4)_n]^{3-2n} + {}^{\bullet}OH + OH^- \quad (9)$$

Moreover, compared to homogenous cases, the reaction mechanisms in such heterogeneous P-FL systems are generally more complex since the whole series of reactions are commonly catalyst surface-limiting. The dominant photochemical reaction (Eq. (4)) could occur not only on the surface of iron oxides heterogeneously but also in the bulk solution homogeneously, while the former initiated and affected strongly the release of dissolved iron species to the bulk solution [12,22]. The adsorbed iron–oxalate complexes of $[Solid{\equiv}Fe^{(III)}(C_2O_4)_n]^{3-2n}$ and $[Solid(Fe^{(II)}(C_2O_4)_n]^{2-2n}$ on the surface of iron oxides and the $[Fe^{(III)}(C_2O_4)_n]^{3-2n}$ and $[Fe^{(II)}(C_2O_4)_n]^{2-2n}$ in the bulk solution could form and coexisted, resulting in the occurrence of in situ H_2O_2 generation reactions and Fenton-like reaction [12].

Regarding the significant synergistic degradation of SMZ achieved in the SP-FL system, the comprehensive effect in the reaction mechanism and enhancement role of US could be addressed separately in two parts: (1) the reaction mechanism on the catalyst surface and in the heterogeneous solid–liquid interphase, and (2) the homogeneous reaction mechanism in the bulk solution. Then,

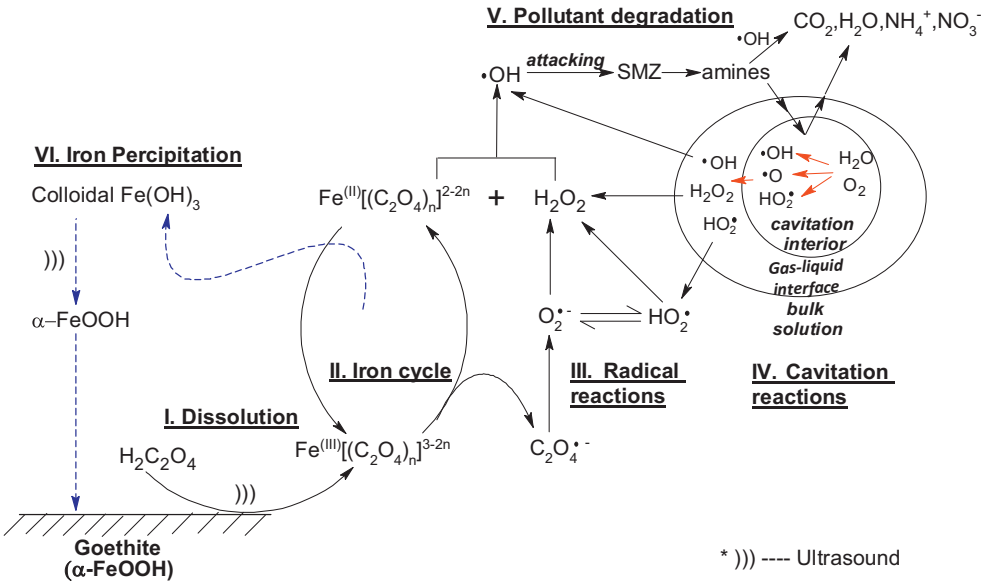

Fig. 7. Proposed scheme of the reaction mechanism and promotional role of US in the SP-FL system.

an integrated reaction mechanism in the SP-FL system as well as the promotional of US is proposed (Fig. 7).

First, US could produce strong mechanical effect in the SP-FL system, including both the significant enhancement in the mass transfer for the solid–liquid interphase reactions and the intensive surface cleaning of the solid (goethite) surface. It have been already verified that US could efficiently accelerate the key rate-limiting steps in many cases, especially in some catalyzed heterogeneous systems [38]. Therefore, it could be concluded that the rate-limiting barrier in the SP-FL system between the solid phase and the bulk solution phase would be easily overcome by US and results in the increasing rates of the whole reaction scheme. In addition, the intensive US irradiation could continuously regenerate the catalyst surface during the reaction. As a result, the photochemical reactions initiated by the adsorbed iron–oxalate complexes, which would play an important role in the P-FL system, could be relegated in the SP-FL system. Nevertheless, the overall photochemical reactions in the SP-FL system would not be retarded, due to the rates of bulk photochemical reactions in the presence of sufficient Fe(II)–oxalate complexes (Fig. 4a) being much higher than that of heterogeneous photochemical reactions [21–23,39].

Second, US might play an important role in the solid reconstruction in the SP-FL system. With the increase of pH and simultaneous decrease of oxalate concentration throughout the reaction, the dissolved iron species would become excessive and could not be maintained totally in the bulk solution. This would lead to the precipitation of colloidal iron species (commonly anonymous $Fe(OH)_3$) [33]. Interestingly, under US irradiation it has been reported that the colloidal $Fe(OH)_3$ could be efficiently transformed to iron minerals of which α-FeOOH (goethite) was a common product [40,41]. Therefore, US irradiation in the SP-FL system would result in not only continuous recovery of the original goethite surface, but also production of new goethite particles.

Third, the sonochemical cavitation could have profound effect on the bulk radical reactions. As indicated above, the formation and amounts of iron–oxalate complexes in a P-FL system would be indispensable for producing H_2O_2 by two ways: (a) Fe(II)–oxalate complexes react with $O_2^{\bullet-}/HO_2^{\bullet}$ to form H_2O_2 (Eq. (8)), and (b) $HO_2^{\bullet}$ reacts with $O_2^{\bullet-}/HO_2^{\bullet}$ to form H_2O_2 by the dismutation (Eq. (7)). Then, a transformation route from $(C_2O_4)^{\bullet-}$ to •OH (i.e. Eqs. (4)–(9)) in the bulk solution based on the key two intermediate radicals ($O_2^{\bullet-}/HO_2^{\bullet}$) could be depicted in Fig. 7.

Ultrasound irradiation can induce the splitting of water molecules with the presence of dissolved oxygen and causes reactions (depicted as Eqs. (10)–(21) below) to occur [42]. In these reactions, '))' denotes the ultrasonic irradiation.

$$H_2O +))) \rightarrow {}^{\bullet}OH + {}^{\bullet}H \quad (10)$$

$$O_2 +))) \rightarrow 2{}^{\bullet}O \quad (11)$$

$${}^{\bullet}O + {}^{\bullet}OH \rightarrow HO_2{}^{\bullet} \quad (12)$$

$${}^{\bullet}O + H_2O \rightarrow 2{}^{\bullet}OH \quad (13)$$

$${}^{\bullet}H + O_2 \rightarrow HO_2{}^{\bullet} \quad (14)$$

$${}^{\bullet}OH + {}^{\bullet}H \rightarrow H_2O \quad (15)$$

$$2{}^{\bullet}OH \rightarrow H_2O + {}^{\bullet}O \quad (16)$$

$$HO_2{}^{\bullet} + {}^{\bullet}OH \rightarrow O_2 + H_2O \quad (17)$$

$$2{}^{\bullet}OH \rightarrow H_2O_2 \quad (18)$$

$$2HO_2{}^{\bullet} \rightarrow H_2O_2 + O_2 \quad (19)$$

$${}^{\bullet}OH + H_2O_2 \rightarrow HO_2{}^{\bullet} + H_2O \quad (20)$$

$${}^{\bullet}H + H_2O_2 \rightarrow {}^{\bullet}OH + H_2O \quad (21)$$

Thermal dissociation of water and dissolved oxygen molecules in the cavities convert them into reactive species such as •OH, •H, and $HO_2^{\bullet}$ in a cavitation bubble (Eqs. (10)–(14)). Thereafter, the reactive radicals lead to a variety of chemical reactions in the gas cavitation bubble and/or in the bulk solution. Due to the presence of the solute (dissolved oxygen), recombination reactions of these primary radicals (Eqs. (15)–(17)) to form H_2O, •O and O_2 could be neglected [43,44]. The final product derived from the sonolysis of water, H_2O_2, is formed outside the hot bubbles or at the cooler interface as a consequence of •OH and $HO_2^{\bullet}$ recombinations (Eqs. (18) and (19) respectively). On the other hand, the •OH and •H radicals may further react with H_2O_2 to produce $HO_2^{\bullet}$ and •OH respectively (Eqs. (20)–(21)). In addition, the radicals $HO_2^{\bullet}$ and •OH may also reach the liquid–bubble interface and be released into the bulk solution. In a summary, H_2O_2, •OH and $HO_2^{\bullet}$ are believed to be the main reactive oxygen species released to the bulk solution when the sonochemical bubbles collapse.

Apparently, the sonochemical cavitation effect would accelerate the radical reactions in the SP-FL system, as indicated in Fig. 7. In

the presence of sufficient Fe(II) species, rapid decomposition of the generated H_2O_2 and production of •OH would be reached. It could be mainly responsible for the significant synergistic degradation of SMZ achieved in the SP-FL system. Furthermore, direct hydrolysis of some organic amine intermediates with low molecule weight would be expected to occur inside the sonochemical bubbles, as indicated by numerous studies [42,45,46].

4. Conclusion

In this study, a novel heterogeneous sonophotolytic Fenton-like (SP-FL) system was developed for the degradation of antibiotic SMZ. Integrating in situ H_2O_2 generation under UV illumination and efficient Fe(II) species regeneration, it was evidenced that the SP-FL system could achieve a significant synergistic degradation of SMZ, along with satisfied improvements in organics mineralization and wastewater detoxification. Based on the characterizations of catalyst surface, evolution of dissolved iron species and reactive species, and identification of degradation intermediates and products, the synergistic role of US in the SP-FL system could be most ascribed to its promotional effect in Fenton-like reaction. A comprehensive scheme to describe the reaction mechanism and the mechanistic roles of US in the SP-FL system has been proposed. Additional results (Fig. S1 in the Supporting Information) have evidenced that the rapid degradation of SMZ as well as decomposition of oxalate could still be achieved in the heterogeneous SP-FL system over five consecutive reaction cycles. It suggested that the catalyst goethite could be reused and the heterogeneous SP-FL system could be an appropriate technology for treatment of wastewater containing pharmaceuticals. Nevertheless, a deeper insight into the reaction mechanism and the reconstruction of goethite under US in the SP-FL system are desired in the future investigation.

Acknowledgements

The authors acknowledge the financial support by Key Project in the National Science & Technology Pillar Program during the Twelfth Five-year Plan Period (No. 2012BAC02B04) and Youth Seed Foundation of Huazhong University of Science and Technology (year 2012). The financial support provided by the National Research Foundation of Singapore through project EWI RFP 0802-11 is also acknowledged.

Appendix A. Supplementary data

Supplementary data associated with this article can be found, in the online version, at http://dx.doi.org/10.1016/j.apcatb.2013.02.004.

References

[1] K. Kümmerer, Chemosphere 75 (2009) 417–434.
[2] K.D. Brown, J. Kulis, B. Thomson, T.H. Chapman, D.B. Mawhinney, Science of the Total Environment 366 (2006) 772–783.
[3] A. Nieto, F. Borrull, R.M. Marcé, E. Pocurull, Journal of Chromatography A 1174 (2007) 125–131.
[4] K. Kümmerer, Chemosphere 75 (2009) 435–441.
[5] M. Klavarioti, D. Mantzavinos, D. Kassinos, Environment International 35 (2009) 402–417.
[6] I. Sirés, E. Brillas, Environment International 40 (2012) 212–229.
[7] K. Hanna, T. Kone, G. Medjahdi, Catalysis Communications 9 (2008) 955–959.
[8] C.Y. Kwan, W. Chu, Water Research 37 (2003) 4405–4412.
[9] R. Matta, K. Hanna, T. Kone, S. Chiron, Chemical Engineering Journal 144 (2008) 453–458.
[10] X. Xue, K. Hanna, C. Despas, F. Wu, N. Deng, Journal of Molecular Catalysis A: Chemical 311 (2009) 29–35.
[11] C.Y. Kwan, W. Chu, Chemosphere 67 (2007) 1601–1611.
[12] Q. Lan, F.B. Li, C.S. Liu, X.Z. Li, Environmental Science and Technology 42 (2008) 7918–7923.
[13] C.E. Noradoun, I.F. Cheng, Environmental Science and Technology 39 (2005) 7158–7163.
[14] T. Zhou, Y. Li, F.-S. Wong, X. Lu, Ultrasonics Sonochemistry 15 (2008) 782–790.
[15] J. Jeong, J. Yoon, Water Research 39 (2005) 2893–2900.
[16] J. He, W. Ma, J. He, J. Zhao, J.C. Yu, Applied Catalysis B 39 (2002) 211–220.
[17] M.E. Balmer, B. Sulzberger, Environmental Science and Technology 33 (1999) 2418–2424.
[18] Y. Zuo, J. Zhan, Atmospheric Environment 39 (2005) 27–37.
[19] Y. Deng, K. Zhang, H. Chen, T. Wu, M. Krzyaniak, A. Wellons, D. Bolla, K. Douglas, Y. Zuo, Atmospheric Environment 40 (2006) 3665–3676.
[20] X. Wang, C. Liu, X. Li, F. Li, S. Zhou, Journal of Hazardous Materials 153 (2008) 426–433.
[21] C. Liu, F. Li, X. Li, G. Zhang, Y. Kuang, Journal of Molecular Catalysis A: Chemical 252 (2006) 40–48.
[22] F.B. Li, X.Z. Li, X.M. Li, T.X. Liu, J. Dong, Journal of Colloid and Interface Science 311 (2007) 481–490.
[23] P. Mazellier, B. Sulzberger, Environmental Science and Technology 35 (2001) 3314–3320.
[24] Y. Zuo, J. Holgne, Environmental Science and Technology 26 (1992) 1014–1022.
[25] L.D. Castro, F.P. Capote, Techniques and Instrumentation in Analytical Chemistry, Elsevier, Amsterdam, Netherlands, 2007, pp. 143–192.
[26] M. Muruganandham, J.S. Yang, J.J. Wu, Industrial and Engineering Chemistry Research 46 (2007) 691–698.
[27] H. Katsumata, T. Okada, S. Kaneco, T. Suzuki, K. Ohta, Ultrasonics Sonochemistry 17 (2010) 200–206.
[28] T. Zhou, T.T. Lim, X. Wu, Water Research 45 (2011) 2915–2924.
[29] B.M. Voelker, B. Sulzberger, Environmental Science and Technology 30 (1996) 1106–1114.
[30] C. Tai, J.-F. Peng, J.-F. Liu, G.-B. Jiang, H. Zou, Analytica Chimica Acta 527 (2004) 73–80.
[31] T. Zhou, T.-T. Lim, Y. Li, X. Lu, F.-S. Wong, Chemosphere 78 (2010) 576–582.
[32] R.M. Cornell, U. Schwertmann, The Iron Oxides, WILEY-VCH GmbH & Co. kGaA, Weinheim, 2003, pp. 172–177.
[33] N. Boonrattanakij, M.-C. Lu, J. Anotai, Water Research 45 (2011) 3255–3262.
[34] G.V. Buxton, C.L. Greenstock, W.P. Helman, A.B. Ross, Journal of Physical and Chemical Reference Data 17 (1988) 513–886.
[35] S. Kaniou, K. Pitarakis, I. Barlagianni, I. Poulios, Chemosphere 60 (2005) 372–380.
[36] P. Calza, C. Medana, M. Pazzi, C. Baiocchi, E. Pelizzetti, Applied Catalysis B 53 (2004) 63–69.
[37] S.P. Mezyk, T.J. Neubauer, W.J. Cooper, J.R. Peller, Journal of Physical Chemistry A 111 (2007) 9019–9024.
[38] Y.G. Adewuyi, Environmental Science and Technology 39 (2005) 8557–8570.
[39] J. Lei, C. Liu, F. Li, X. Li, S. Zhou, T. Liu, M. Gu, Q. Wu, Journal of Hazardous Materials 137 (2006) 1016–1024.
[40] N. Enomoto, J.-i. Akagi, Z.-e. Nakagawa, Ultrasonics Sonochemistry 3 (1996) S97–S103.
[41] M.D. Luque de Castro, F. Priego-Capote, Ultrasonics Sonochemistry 14 (2007) 717–724.
[42] L.H. Thompson, L.K. Doraiswamy, Industrial and Engineering Chemistry Research 38 (1999) 1215–1249.
[43] M. Ashokkumar, J. Lee, S. Kentish, F. Grieser, Ultrasonics Sonochemistry 14 (2007) 470–475.
[44] H. Yanagida, Ultrasonics Sonochemistry 15 (2008) 492–496.
[45] A. Kamal, S.F. Adil, M. Arifuddin, Ultrasonics Sonochemistry 12 (2005) 429–431.
[46] Y.G. Adewuyi, Industrial and Engineering Chemistry Research 40 (2001) 4681–4715.